In Vitro Model for a Drug Assessment of Cytochrome P450 Family 3 Subfamily A Member 4 Substrates Using Human Induced Pluripotent Stem Cells and Genome Editing Technology

Sayaka Deguchi,[1] Tomohiro Shintani,[1] Kazuo Harada,[2] Toru Okamoto,[3] Akinori Takemura,[4] Kazumasa Hirata,[2] Kousei Ito,[4] Kazuo Takayama,[1,5] and Hiroyuki Mizuguchi[1,6-8]

In drug development, a system for predicting drug metabolism and drug-induced toxicity is necessary to ensure drug safety. Cytochrome P450 family 3 subfamily A member 4 (CYP3A4) is an important drug-metabolizing enzyme expressed in the liver and small intestine, and predicting CYP3A4-mediated drug metabolism and drug-induced toxicity is essential. We previously developed procedures to differentiate human induced pluripotent stem (iPS) cells into hepatocyte-like cells (HLCs) or intestinal epithelial-like cells (IECs) with a fetal phenotype as well as a highly efficient genome editing technology that could enhance the homologous recombination efficiency at any locus, including CYP3A4. By using human iPS cells and our genome editing technology, we generated CYP3A4-knockout (KO) iPS cell-derived HLCs and IECs for the evaluation of CYP3A4-mediated drug metabolism and drug-induced toxicity. CYP3A4 deficiency did not affect pluripotency and hepatic and intestinal differentiation capacities, and CYP3A4 activity was entirely eradicated by CYP3A4 KO. Off-target effects (e.g., inhibition of bile acid excretion) were hardly observed in CYP3A4-KO cells but were observed in CYP3A4 inhibitor-treated (e.g., ketoconazole) cells. To evaluate whether drug-induced hepatotoxicity and enterotoxicity could be predicted using our model, we exposed CYP3A4-KO HLCs and IECs to acetaminophen, amiodarone, desipramine, leflunomide, tacrine, and tolcapone and confirmed that these cells could predict CYP3A4-mediated toxicity. Finally, we examined whether the therapeutic effects of an anti-hepatitis C virus (HCV) drug metabolized by CYP3A4 would be predicted using our model. CYP3A4-KO HLCs were treated with asunaprevir (antiviral drug metabolized by CYP3A4) after HCV infection, and the anti-viral effect was indeed strengthened by CYP3A4 KO. *Conclusion*: We succeeded in generating a novel evaluation system for prediction of CYP3A4-mediated drug metabolism and drug-induced toxicity. (*Hepatology Communications* 2021;5:1385-1399).

In drug development, ensuring the safety of drugs is an important issue, and it is therefore necessary to predict drug metabolism and drug-induced toxicity at an early stage of preclinical studies. Cytochrome P450 family 3 subfamily A member 4 (CYP3A4), a major drug-metabolizing enzyme highly

Abbreviations: AAT, alpha-1 antitrypsin; ALB, albumin; ASV, asunaprevir; BA, bile acid; BEI, biliary excretion index; BSEP, bile salt export pump; CRISPR, clustered regularly interspaced short palindromic repeats; CYP3A4, cytochrome P450 family 3 subfamily A member 4; DAA, direct-acting antiviral; DAPI, 4′,6-diamidino-2-phenylindole; DMSO, dimethyl sulfoxide; FACS, fluorescence-activated cell sorting; HCV, hepatitis C virus; HLC, hepatocyte-like cell; IEC, intestinal epithelial-like cell; iPS cell, induced pluripotent stem cell; kb, kilobase; kbp, kilobase pair; KO, knockout; MPS, microphysiological system; NS, nonstructural protein; OCT3/4, POU domain, class 5, transcription factor 1; PCR, polymerase chain reaction; RT-PCR, reverse-transcription polymerase chain reaction; sgRNA, single guide RNA; SOX2, sex determining region Y-box 2; UPLC/MS-MS, ultra-performance liquid chromatography–tandem mass spectrometry; WT, wild type.

Received April 22, 2020; accepted March 19, 2021.

Additional Supporting Information may be found at onlinelibrary.wiley.com/doi/10.1002/hep4.1729/suppinfo.

Supported by the Japan Agency for Medical Research and Development (grants 19be0304320h0003 to K.T., 19mk0101125h0002 to K.T., 19fk0210021h0003 to H.M., 19fk0210055h0001 to T.O., 20mk0101125h0003 to K.T., and 20be0304202h0004 to K.T.), Mochida Memorial Foundation for Medical and Pharmaceutical Research to K.T., and Uehara Memorial Foundation to H.M.

expressed in the liver and the small intestine, metabolizes almost half of commercially available drugs.[1] Drug–drug interactions mediated by CYP3A4 have a risk of causing side effects or therapeutic effects from a wide range of drugs. Therefore, an *in vitro* system to evaluate CYP3A4-mediated drug metabolism and toxicity is required. In general, drug metabolism and toxicity are examined by using CYP3A4 inhibitor-treated carcinoma cell lines or microsomes. However, this evaluation system has several problems. The drug-metabolizing capacity in some carcinoma cell lines (such as HepG2 or Huh7.5.1 cells, except HepaRG cells) is low, and their properties are different from those of normal human hepatocytes. Microsomes do not contain drug-metabolizing enzymes expressed in the cytosol, such as glutathione S-transferase or sulfotransferase. In addition, it is difficult to develop an isoform-selective CYP inhibitor because the amino acid sequences of CYP isoforms are similar to each other. For the above reasons, it is still hard to generate *in vitro* evaluation systems that can faithfully reproduce drug metabolism and drug-induced toxicity *in vivo*.

Human induced pluripotent stem (iPS) cell derivatives are now being used or considered in drug development. We have developed procedures to efficiently differentiate human iPS cells into hepatocyte-like cells (HLCs) and intestinal epithelial-like cells (IECs).[2-5] Because our human iPS cell-derived HLCs and IECs possess high drug-metabolizing activity, they would be a suitable model for the evaluation of drug metabolism and drug-induced toxicity. In addition, functions of human iPS cell-derived HLCs and IECs can be maintained for more than a week, while primary human hepatocytes and intestinal epithelial cells rapidly lose their function after cell plating. We have also developed an efficient genome editing technology for human iPS cells, using the clustered regularly interspaced short palindromic repeats (CRISPR)-Cas9 system.[6] Although it is known that the homologous recombination efficiency in transcriptionally inactive genes is low, our unique genome editing technology could enhance homologous recombination efficiency regardless of the transcriptional activity of the targeted genes, including drug-metabolizing

View this article online at wileyonlinelibrary.com.
DOI 10.1002/hep4.1729
Potential conflict of interest: Nothing to report.

ARTICLE INFORMATION:

From the [1]Laboratory of Biochemistry and Molecular Biology, Graduate School of Pharmaceutical Sciences, Osaka University, Osaka, Japan; [2]Laboratory of Applied Environmental Biology, Graduate School of Pharmaceutical Sciences, Osaka University, Osaka, Japan; [3]Institute for Advanced Co-creation Studies, Research Institute for Microbial Diseases, Osaka University, Osaka, Japan; [4]Laboratory of Biopharmaceutics, Graduate School of Pharmaceutical Sciences, Chiba University, Chiba, Japan; [5]Center for Induced Pluripotent Stem Cell Research and Application, Kyoto University, Kyoto, Japan; [6]Laboratory of Hepatocyte Regulation, National Institutes of Biomedical Innovation, Health and Nutrition, Osaka, Japan; [7]Global Center for Medical Engineering and Informatics, Osaka University, Osaka, Japan; [8]Integrated Frontier Research for Medical Science Division of the Institute for Open and Transdisciplinary Research Initiatives, Osaka University, Osaka, Japan.

ADDRESS CORRESPONDENCE AND REPRINT REQUESTS TO:

Kazuo Takayama, Ph.D.
Laboratory of Biochemistry and Molecular Biology
Graduate School of Pharmaceutical Sciences, Osaka University
1-6 Yamadaoka
Suita, Osaka 565-0871, Japan
E-mail: takayama@phs.osaka-u.ac.jp
Tel.: +81-6-6879-8187
or

Hiroyuki Mizuguchi, Ph.D.
Laboratory of Biochemistry and Molecular Biology
Graduate School of Pharmaceutical Sciences, Osaka University
1-6 Yamadaoka
Suita, Osaka 565-0871, Japan
E-mail: mizuguch@phs.osaka-u.ac.jp
Tel.: +81-6-6879-8185

enzymes or drug transporters.[7-9] Therefore, if we succeed in generating CYP3A4-knockout (KO) iPS cell-derived HLCs and IECs, it would be possible to evaluate CYP3A4-mediated drug metabolism and drug-induced toxicity selectively *in vitro*.

In this study, we established CYP3A4-KO iPS cells by using our unique genome editing technology and differentiated them into HLCs (CYP3A4-KO HLCs) and IECs (CYP3A4-KO IECs). To examine whether these cells could predict CYP3A4-mediated drug metabolism and drug-induced toxicity, we performed a drug metabolism test and drug-induced toxicity test using typical drugs. Additionally, we compared our model with the existing model using ketoconazole, which is widely used as a CYP3A4 inhibitor, and confirmed that our model is more specific to CYP3A4.

Materials and Methods

ELECTROPORATION

The *CYP3A4* locus was targeted using the donor plasmids and CRISPR-Cas9 plasmids. The plasmids expressing *Streptococcus pyogenes* Cas9 (SpCas9) and single guide RNA (sgRNA) were generated by ligating double-stranded oligonucleotides into the *Bbs*I site of pX330 (Addgene no. 42230; http://www.addgene.org/42230/).[10] The sgRNA sequences are shown in Supporting Table S1. Donor plasmids were generated by conjugating the following four fragments: two homology arms (1.04 kilobase [kb] for both the 3′ arm and 5′ arm), an elongation factor 1α (EF1α)-puromycin resistance (PuroR)-pA cassette, and linearized backbone plasmids (pENTR donor plasmids). The backbone plasmids were the kind gift of Dr. Akitsu Hotta (Center for iPS Cell Research and Application, Kyoto University).[11] The efficient targeting experiments of human iPS cells were performed as described.[6] Briefly, human iPS cells were treated with 10 μM valproic acid for 24 hours. Human iPS cells (1.0×10^6 cells) were dissociated into single cells by using TrypLE Select Enzyme and resuspended in Opti-MEM (Thermo Fisher Scientific). Electroporation was performed by using a NEPA21 electroporator (Nepa Gene) according to the manufacturer's instructions. The ratio of Opti-MEM solution to the plasmid solution was 90 μL:22 μL (total 112 μL). The plasmid solution consisted of 5 μg donor plasmids, 15 μg CRISPR-Cas9 plasmids (three CRISPR-Cas9 vectors carrying different sgRNAs were mixed), and 2 μg RAD51 recombinase (RAD51)-expressing plasmids. After electroporation, the cells were seeded onto 1-μg/cm^2 iMatrix-511-coated dishes and cultured with StemFit AK02N medium containing 10 μM Rho-associated protein kinase (ROCK) inhibitor. After culturing for 2 days, the medium was replaced with 20 μM puromycin-containing medium. Then, 48 hours after its addition, the puromycin-containing medium was removed and the original medium was added. At 14 days after electroporation, 30 individual colonies were picked up and then seeded onto a 1-μg/cm^2 iMatrix-511-coated six-well plate. After most of the wells became nearly confluent, polymerase chain reaction (PCR) was performed to examine whether the clones were correctly targeted.

REAL-TIME RT-PCR

ISOGEN (NIPPON GENE) was used to isolate total RNA from the cells. A Superscript VILO cDNA synthesis kit (Thermo Fisher Scientific) was used to synthesize cDNA from 500 ng of the isolated total RNA. Real-time RT-PCR was performed with SYBR Green PCR Master Mix (Thermo Fisher Scientific) using a StepOnePlus real-time PCR system (Thermo Fisher Scientific). The $2^{-\Delta\Delta CT}$ method was adopted for the relative quantitation of target mRNA levels. The values of the target genes were normalized by those of the housekeeping gene, glyceraldehyde 3-phosphate dehydrogenase (*GAPDH*). The PCR primer sequences (described in Supplementary Table 2) used in this report were obtained from PrimerBank (https://pga.mgh.harvard.edu/primerbank/).

IMMUNOHISTOCHEMISTRY

The human iPS cells and their derivatives were fixed with 4% paraformaldehyde in PBS at 4°C for 15 min. After blocking the cells with PBS containing 2% bovine serum albumin and 0.2% Triton X-100 at room temperature for 45 min, the cells were incubated with a primary antibody at 4°C overnight, and then with a secondary antibody at room temperature for 1 hr. All antibodies used in this report are described in Supplementary Table 3.

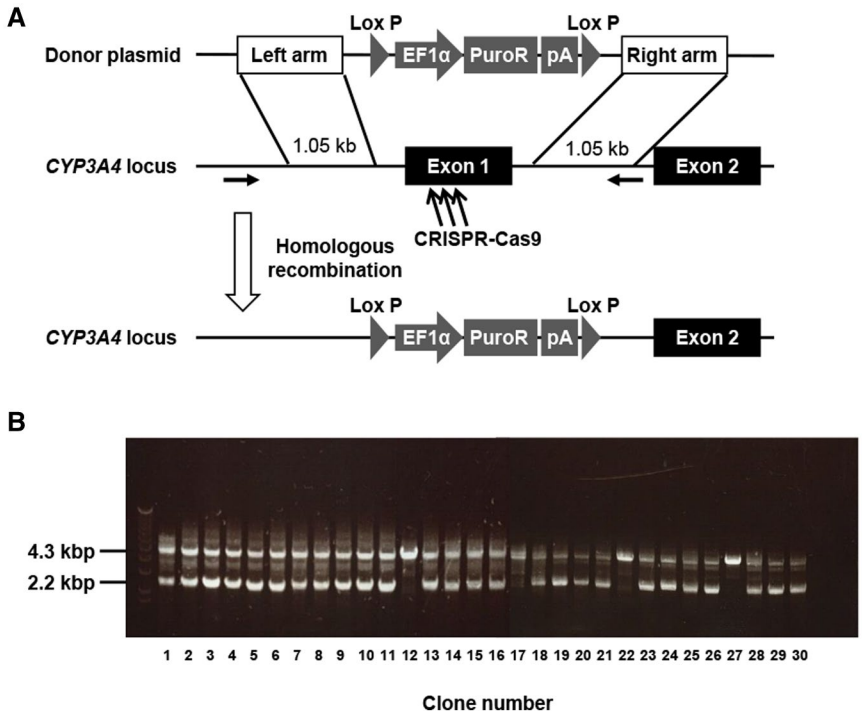

FIG. 1. Establishment of CYP3A4-KO human iPS cells. (A) Schematic overview of the targeting strategy for CYP3A4 is shown. PCR primers that can distinguish WT and mutant alleles are shown with arrows. (B) Genotyping was performed to examine whether the human iPS cell clones were correctly targeted. Abbreviations: EF1α, elongation factor 1α; Lox P, locus of X-over P1; PuroR, puromycin resistance.

FLOW CYTOMETRY

Single-cell suspensions of human iPS cell-derived cells were fixed with 4% paraformaldehyde (PFA) at 4°C for 10 min, and then incubated with the primary antibodies, followed by the secondary antibodies. Analysis was performed on a MACSQuant Analyzer (Miltenyi Biotec) and FlowJo software (FlowJo LLC, http://www.flowjo.com/). All antibodies used in this report are described in Supplementary Table 4.

ASSESSMENT OF DRUG-INDUCED CELL TOXICITY

Wild-type (WT) and CYP3A4-KO HLCs were exposed to different concentrations of acetaminophen (FUJIFILM Wako), amiodarone (TCI Chemicals), desipramine (FUJIFILM Wako), tacrine (Sigma), tolcapone (Sigma), or leflunomide (Sigma) for 4 days. Cell viability was examined by a WST-8 assay, using a Cell Counting Kit-8 purchased from Dojindo Laboratories. The WST-8 assay was performed according to the manufacturer's instructions. Cell viability was calculated as a percentage of the viability of cells treated with vehicle (dimethyl sulfoxide [DMSO]) only.

Results

ESTABLISHMENT OF CYP3A4-KO HUMAN iPS CELLS

To establish CYP3A4-KO iPS cells, we designed donor plasmids targeting CYP3A4 (Fig. 1A). We used sgRNA/SpCas9 co-expressing plasmids (pX330) and RAD51-expressing plasmids with donor plasmids to perform efficient, homologous, recombination-mediated gene editing at the *CYP3A4* locus in human iPS cells. Human iPS cells were electroporated with these plasmids. After positive selection with puromycin, we obtained 30 human iPS cell colonies. Genomic DNA was extracted and genotyping analysis was performed

using the primers indicated by arrows in Fig. 1A in order to examine whether the obtained human iPS cell colonies carry the transgene cassette at the targeted locus. PCR primers were designed to distinguish WT and mutant alleles; WT cells show a 2.2 kilobase pair (kbp) band, biallelically targeted cells show a 4.3 kbp band, and monoallelically targeted cells show both bands (2.2 and 4.3 kbp bands). Four human iPS cell clones (numbers 12, 17, 22, and 27) were biallelically targeted at the *CYP3A4* locus (Fig. 1B). From this result, we succeeded in establishing human iPS cells with a defect in exon 1 of the *CYP3A4* gene, which includes its start codon.

PLURIPOTENCY OF CYP3A4-KO HUMAN iPS CELLS

We examined whether the pluripotency of CYP3A4-KO iPS cells is similar to that of WT iPS cells (Fig. 2). Phase images showed no morphologic difference between WT iPS cells and CYP3A4-KO iPS cells (Fig. 2A). Real-time reverse-transcription (RT) PCR analysis showed that the gene expression levels of pluripotent markers (nanog homeobox [*NANOG*], POU domain, class 5, transcription factor 1 [*OCT3/4*], and sex determining region Y-box 2 [*SOX2*]) were not changed by CYP3A4 KO (Fig. 2B). Immunostaining analysis also showed that protein expression levels of OCT3/4 and SOX2 were not changed by CYP3A4 KO (Fig. 2C). In addition, both WT iPS cells and CYP3A4-KO iPS cells showed normal karyotypes (Fig. 2D). The pluripotency of WT iPS cells and CYP3A4-KO iPS cells was also evaluated using the teratoma formation assay (Fig 2E). We confirmed that both WT iPS cell-derived and CYP3A4-KO iPS cell-derived teratomas were composed of derivatives of all three embryonic germ layers (ectoderm, mesoderm, and endoderm). Taken together, these results suggest that CYP3A4 deficiency does not affect the pluripotency of human iPS cells.

HEPATIC DIFFERENTIATION CAPACITY OF CYP3A4-KO HUMAN iPS CELLS

CYP3A4 is highly expressed in the liver, and many drugs are known to be metabolized by CYP3A4 in the liver. Also, some drugs that are substrates for CYP3A4 cause hepatotoxicity, which is the most common reason for drug withdrawal from the market.[12] Therefore, we attempted to establish CYP3A4-KO HLCs. To examine whether the hepatic differentiation capacity of CYP3A4-KO iPS cells is similar to that of WT iPS cells, both WT iPS cells and CYP3A4-KO iPS cells were differentiated into HLCs, as described in Fig. 3A, and then the gene expression levels of hepatic markers in WT HLCs and CYP3A4-KO HLCs were examined (Fig. 3B). Gene expression levels of albumin (*ALB*), alpha-fetoprotein (*AFP*), alpha-1 antitrypsin (*AAT*), transthyretin (*TTR*), hepatocyte nuclear factor 4 alpha (*HNF4A*), *CYP2B6*, bile salt export pump (*BSEP*), aldolase, fructose-bisphosphate B (*ALDOB*), constitutive androstane receptor (*CAR*), multidrug resistance-associated protein 2 (*MRP2*), and pregnane X receptor (*PXR*) in CYP3A4-KO HLCs were similar to those in WT HLCs. Enzyme-linked immunosorbent assay analysis showed that ALB secretion capacity was not changed by CYP3A4 KO (Fig. 3C). We also measured the percentage of CYP3A4-positive cells in the WT HLCs and CYP3A4-KO HLCs by using fluorescence-activated cell sorting (FACS) analysis (Fig. 3D). The percentage of CYP3A4-positive cells was significantly decreased in CYP3A4-KO HLCs compared with WT HLCs. Immunostaining analysis also showed that the protein expression levels of ALB and AAT were not changed by CYP3A4 KO (Fig. 3E). To examine the global gene expression profiles in WT HLCs and CYP3A4-KO HLCs, RNA sequence analysis was performed (Fig. 3F). Gene expression of *CYP3A4* almost disappeared in CYP3A4-KO HLCs, and there was little difference in gene expression levels of most genes (>97%) between WT HLCs and CYP3A4-KO HLCs (Fig. 3F). In addition, the expression signal values of the 393 genes that had a similar sequence to the sgRNA target sequences were extracted from the data generated by RNA sequence analysis (Supporting Fig. S1). This result suggests that there were no detectable off-target effects by CRISPR-Cas9-derived RNA-guided endonucleases. Taken together, these results indicate that CYP3A4 deficiency does not affect the hepatic differentiation capacity of human iPS cells.

DRUG-METABOLIZING CAPACITY OF CYP3A4-KO HUMAN iPS CELL-DERIVED HLCs

We performed ultra-performance liquid chromatography–tandem mass spectrometry (UPLC/

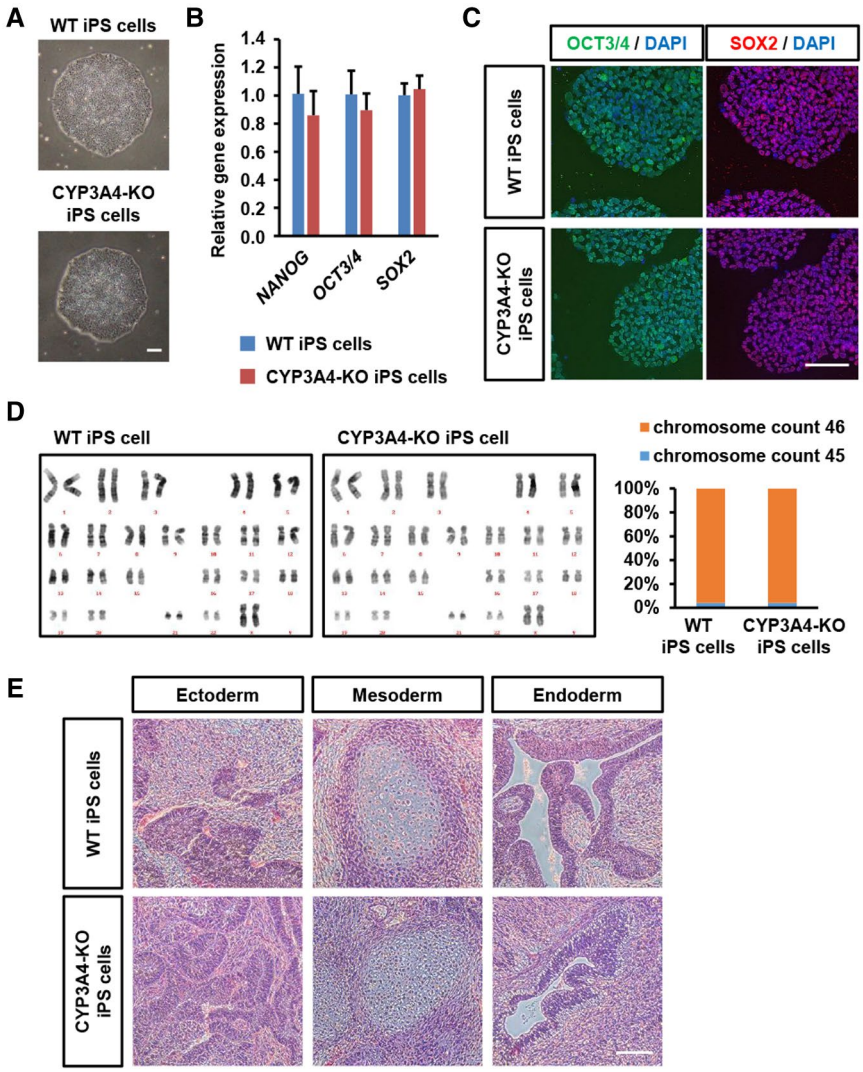

FIG. 2. Pluripotent capacity of CYP3A4-KO human iPS cells. (A) Phase contrast images of WT iPS cells and CYP3A4-KO iPS cells are shown. Scale bar, 100 μm. (B) Gene expression levels of *NANOG*, *OCT3/4*, and *SOX2* in WT iPS cells and CYP3A4-KO iPS cells were measured by real-time RT-PCR analysis. Gene expression levels in WT iPS cells were taken as 1.0. Data represent mean ± SD (n = 3). (C) WT iPS cells and CYP3A4-KO iPS cells were subjected to immunostaining with anti-OCT3/4 (green) and anti-SOX2 (red) antibodies. Nuclei were counterstained with DAPI (blue). Scale bar, 100 μm. (D) Chromosomal Q-band analyses were performed in WT iPS cells and CYP3A4-KO iPS cells. (E) A teratoma formation assay was performed in WT iPS cells and CYP3A4-KO iPS cells using *Rag2/Il2rg* double-knockout mice. At 8 weeks after the transplantation, teratomas were collected and hematoxylin and eosin staining was performed. Scale bar, 100 μm. Abbreviations: *Il2rg*, interleukin 2 receptor subunit gamma; NANOG, nanog homeobox; *Rag2*, recombination activating 2.

MS-MS) analysis to compare the CYP3A4-mediated drug-metabolizing capacity in WT HLCs and CYP3A4-KO HLCs (Fig. 4A). As we noted previously, ketoconazole is widely used as a potent CYP3A4 inhibitor. Therefore, the CYP3A4-mediated drug-metabolizing capacity in ketoconazole-treated HLCs was also evaluated. WT HLCs, ketoconazole-treated WT HLCs, and CYP3A4-KO HLCs were treated with midazolam, which is known as a substrate of CYP3A4, and the quantity of 1′-hydroxymidazolam, which is the metabolite of midazolam, was measured by UPLC/MS-MS analysis. CYP3A4 metabolic activity was significantly lower in CYP3A4-KO HLCs than in WT HLCs and ketoconazole-treated WT HLCs (WT HLCs, 1.7×10^3 pmol/hour/mg protein; ketoconazole-treated WT HLCs, 5.3×10^2 pmol/hour/mg protein;

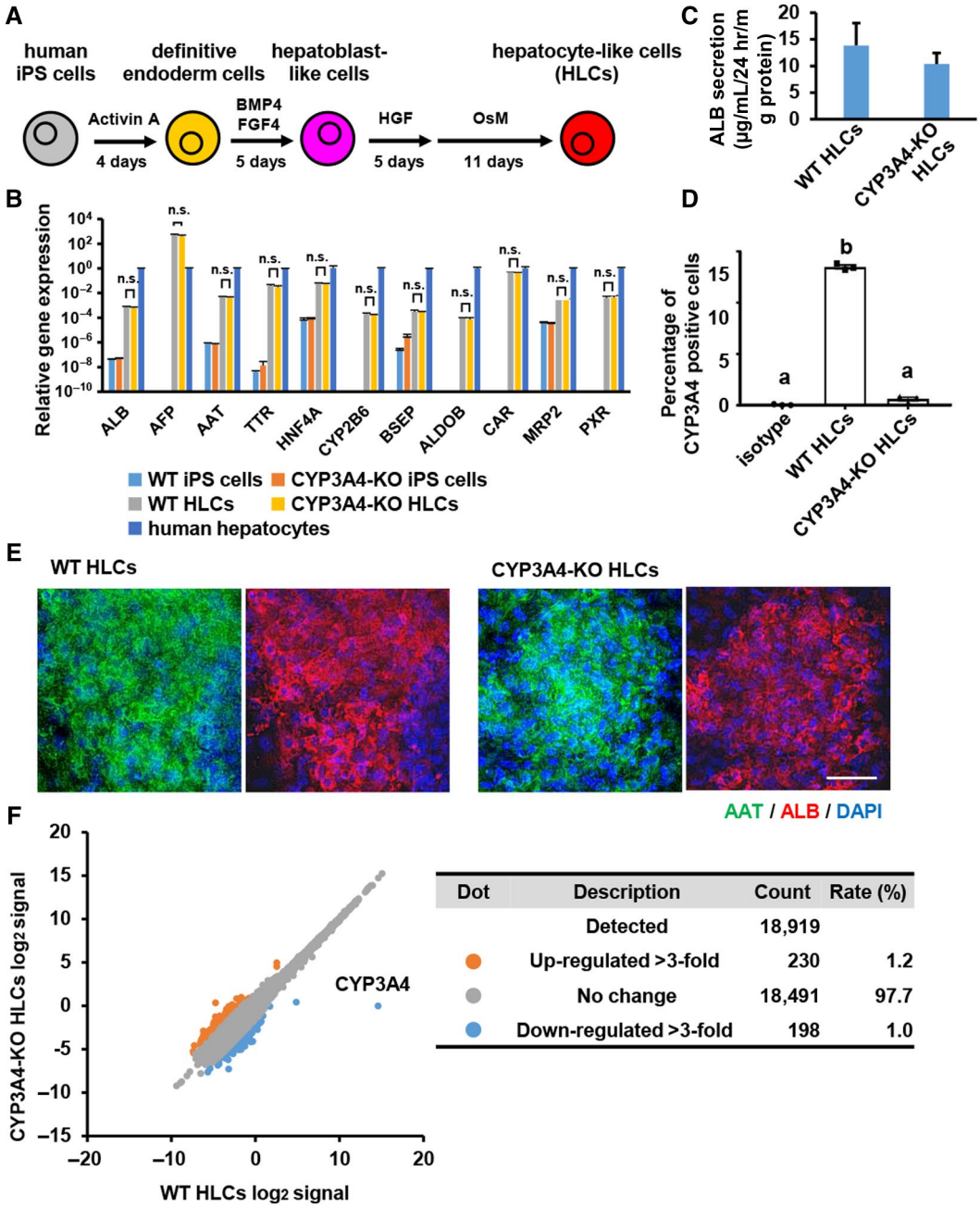

FIG. 3. Hepatic differentiation capacity of CYP3A4-KO human iPS cells. (A) Schematic overview shows the protocol for hepatic differentiation. (B) Gene expression levels of hepatic markers were examined using real-time RT-PCR in WT iPS cells, CYP3A4-KO iPS cells, WT HLCs, CYP3A4-KO HLCs, and human hepatocytes immediately after thawing. Gene expression levels in human hepatocytes were taken as 1.0. (C) Amounts of ALB secretion in WT HLCs and CYP3A4-KO HLCs were examined by ELISA. (D) Percentage of CYP3A4-positive cells in the WT HLCs and CYP3A4-KO HLCs was measured by using FACS analysis. Groups that do not share the same letter are significantly different from each other ($P < 0.05$, Tukey's post hoc tests). (E) WT HLCs and CYP3A4-KO HLCs were subjected to immunostaining with anti-AAT (green) and anti-ALB (red) antibodies. Nuclei were counterstained with DAPI (blue). Scale bar, 50 μm. (F) RNA sequence analysis was performed in WT HLCs and CYP3A4-KO HLCs. A scatter plot of the gene expression signals in both cells is shown. Red dots and blue dots indicate the genes whose expression levels were up- and down-regulated more than 3-fold, respectively. All data represent mean ± SD (n = 3). Abbreviations: AFP, alpha-fetoprotein; ALDPB, aldolase, fructose-bisphosphate B; BMP4, bone morphogenetic protein 4; CAR, constitutive androstane receptor; ELISA, enzyme-linked immunosorbent assay; FGF4, fibroblast growth factor 4; HGF, hepatocyte growth factor; HNF4A, hepatocyte nuclear factor 4 alpha; hr, hour; MRP2, multidrug resistance-associated protein 2; n.s., not significant; OsM, oncostatin M; PXR, pregnane X receptor; TTR, transthyretin.

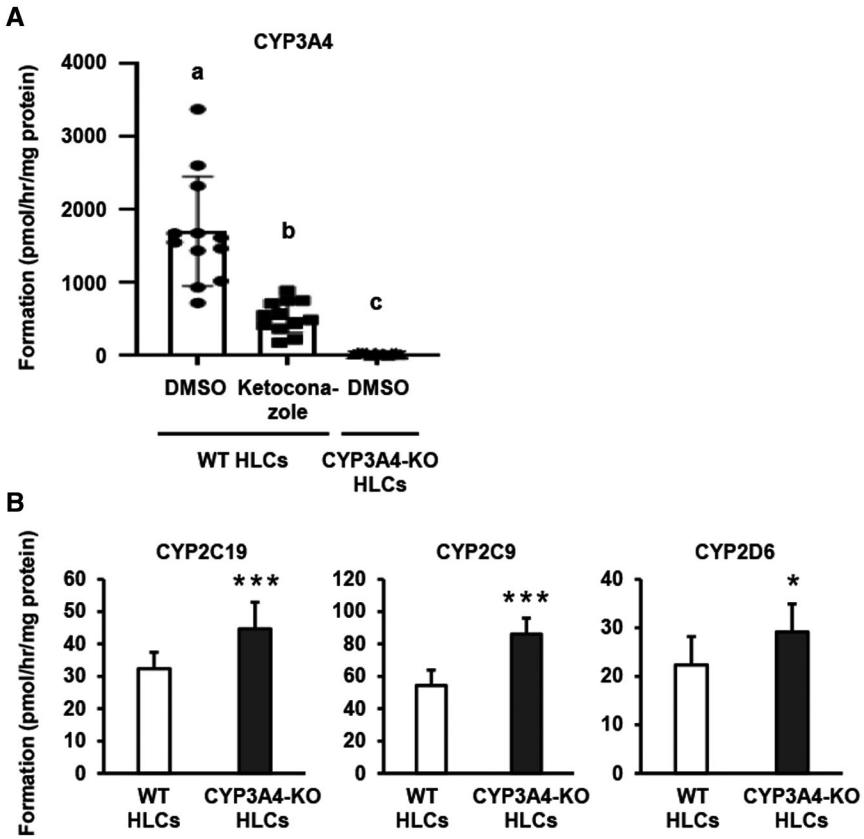

FIG. 4. Drug-metabolizing capacities of CYP3A4-KO HLCs. (A) HLCs were treated with vehicle (DMSO) or ketoconazole (a CYP3A4 inhibitor) for 24 hours. The CYP3A4-mediated drug-metabolizing capacity in WT HLCs and CYP3A4-KO HLCs was evaluated by quantifying the metabolites of midazolam. The quantity of metabolites (1′-hydroxymidazolam) was measured by UPLC/MS-MS. Groups that do not share the same letter are significantly different from each other ($P < 0.05$, Tukey's post hoc tests). (B) CYP-mediated drug-metabolizing capacities in WT HLCs and CYP3A4-KO HLCs were also evaluated by quantifying metabolites of *S*-mephenytoin, diclofenac, and bufuralol. The quantity of metabolites (4′-hydoroxymephenytoin, 4′-hydroxydiclofenac, and 1′-hydroxybufuralol, respectively) was measured by UPLC/MS-MS ($^{*}P < 0.05$, $^{**}P < 0.01$, $^{***}P < 0.005$, Student's *t*-test). All data represent mean ± SD (n = 12). Abbreviation: hr, hour.

CYP3A4-KO HLCs, 2.9 × 10 pmol/hour/mg protein). This result indicates that CYP3A4-KO HLCs do not have CYP3A4-mediated drug-metabolizing capacity.

WT HLCs and CYP3A4-KO HLCs were also treated with *S*-mephenytoin, diclofenac, and bufuralol to examine the drug-metabolizing capacity of CYP2C19, CYP2C9, and CYP2D6, respectively (Fig. 4B). The quantity of metabolites (4′-hydoroxymephenytoin, 4′-hydroxydiclofenac, and 1′-hydroxybufuralol, respectively) was measured by UPLC/MS-MS analysis. CYP2C19, CYP2C9, and CYP2D6 metabolic activities in CYP3A4-KO HLCs were slightly higher than these activities in WT HLCs. This result indicates that the drug-metabolizing capacities of CYP2C19, CYP2C9, and CYP2D6 were compensatorily enhanced by CYP3A4 KO. Similar phenomena could also be observed in Cyp3a-KO mice.[13]

OFF-TARGET EFFECT OF KETOCONAZOLE

Some drugs, such as ketoconazole or itraconazole, are currently used as potent CYP3A4 inhibitors. However, evaluations using an inhibitor are not sufficiently accurate because there are risks of off-target effects. In this study, we focused on biliary excretion capacity and cholestatic liver injury because it is important to distinguish CYP3A4-mediated drug-induced liver injury from cholestatic liver injury. Cholestatic liver injury, which accounts for approximately 40%

of drug-induced liver injury, is often caused by inhibition of biliary excretion. Some reports have shown that ketoconazole inhibits bile acid (BA) transporters, such as BSEP.[14,15] Therefore, we conducted the following experiments to confirm that CYP3A4-KO HLCs would not affect biliary excretion capacity. We also attempted to predict CYP3A4-mediated drug-induced liver injury without an off-target effect.

We observed typical bile canaliculi in both WT HLCs and CYP3A4-KO HLCs (Supporting Fig. S3A). To evaluate the biliary excretion capacity, the biliary excretion index (BEI) was calculated in WT HLCs and CYP3A4-KO HLCs (Fig. 5A). Importantly, the BEI was decreased by ketoconazole treatment, while that was not affected by CYP3A4-KO. Then, to evaluate BA-dependent cholestatic liver injury, WT HLCs and CYP3A4-KO HLCs were exposed to a BA mixture (at 175-fold human serum concentration, described in Supporting Table S5) for 24 hours (Fig. 5B).[16,17] Although ketoconazole treatment did not decrease the cell viability of WT HLCs in the absence of the BA mixture (Supporting Fig. S2B), the treatment did decrease cell viability in the presence of the BA mixture (Fig. 5B). We could observe similar results by using cyclosporine A, a hepatobiliary transport inhibitor (Fig. 5C,D). These results suggest that ketoconazole carries a risk of cholestatic liver injury in the presence of BA. Taken together, our findings indicate that CYP3A4-KO HLCs could predict CYP3A4-mediated drug-induced hepatotoxicity because, unlike ketoconazole-treated cells, CYP3A4-KO HLCs could distinguish CYP3A4-mediated drug-induced liver injury from cholestatic liver injury.

PREDICTION OF DRUG-INDUCED LIVER INJURY USING HUMAN iPS CELL-DERIVED HLCs

To examine whether CYP3A4-KO HLCs could be used in the prediction of drug-induced liver injury, WT HLCs and CYP3A4-KO HLCs were treated with six hepatotoxic drugs and their cell viability was measured 4 days later (Fig. 6). Acetaminophen, amiodarone, desipramine, tacrine, and tolcapone are reportedly metabolized by CYP3A4 and carry a risk of hepatotoxicity.[18-22] Leflunomide is mainly metabolized by CYP2C9.[23] When these cells were treated with acetaminophen, desipramine, tacrine, or tolcapone, cell viabilities were significantly higher in CYP3A4-KO HLCs than in WT HLCs. Additionally, the decrease in hepatotoxicity in acetaminophen-treated CYP3A4-KO HLCs was cancelled by CYP3A4 Supersomes treatment (Supporting Fig. S3). On the other hand, cell viabilities of CYP3A4-KO HLCs and WT HLCs were similar when these cells were treated with amiodarone and leflunomide. These results suggest that CYP3A4-KO HLCs would be useful for predicting CYP3A4-mediated hepatotoxicity of some drugs.

CHARACTERIZATION OF CYP3A4-KO HUMAN iPS CELL-DERIVED IECs

CYP3A4 is also a major CYP expressed in the small intestine as well as the liver. Thus, it is necessary to examine CYP3A4-mediated drug metabolism in both these organs. Here, we tried to establish CYP3A4-KO IECs. Both WT iPS cells and CYP3A4-KO iPS cells were differentiated into IECs, as described in Fig. 7A. First, the intestinal differentiation capacity of WT iPS cells and CYP3A4-KO iPS cells was examined (Fig. 7B-D). Immunostaining analysis showed that protein expression levels of villin were not changed by CYP3A4 KO (Fig. 7B). Gene expression levels of intestinal markers (villin, sucrase-isomaltase [*SI*], caudal type homeobox 2 [*CDX2*], and breast cancer resistance protein [*BCRP*]) were also not changed by CYP3A4 KO (Fig. 7C). Additionally, FACS analysis showed that the percentage of villin-positive cells in CYP3A4-KO IECs was similar to that in WT IECs (Fig. 7D). These results suggest that CYP3A4 deficiency does not affect the intestinal differentiation capacity of human iPS cells. Secondly, we examined CYP3A4 expression levels and CYP3A4-mediated drug-metabolizing capacity in CYP3A4-KO IECs. FACS analysis showed that the percentage of CYP3A4-positive cells was significantly decreased in CYP3A4-KO IECs compared with WT IECs (Fig. 7E). To compare the CYP3A4-mediated drug-metabolizing capacity among WT IECs, ketoconazole-treated WT IECs, and CYP3A4-KO IECs, UPLC/MS-MS analysis was performed, and the amount of the metabolite of midazolam (1′-hydroxymidazolam) was measured (Fig. 7F). The metabolic activity in CYP3A4-KO IECs was lower than in WT IECs and ketoconazole-treated WT

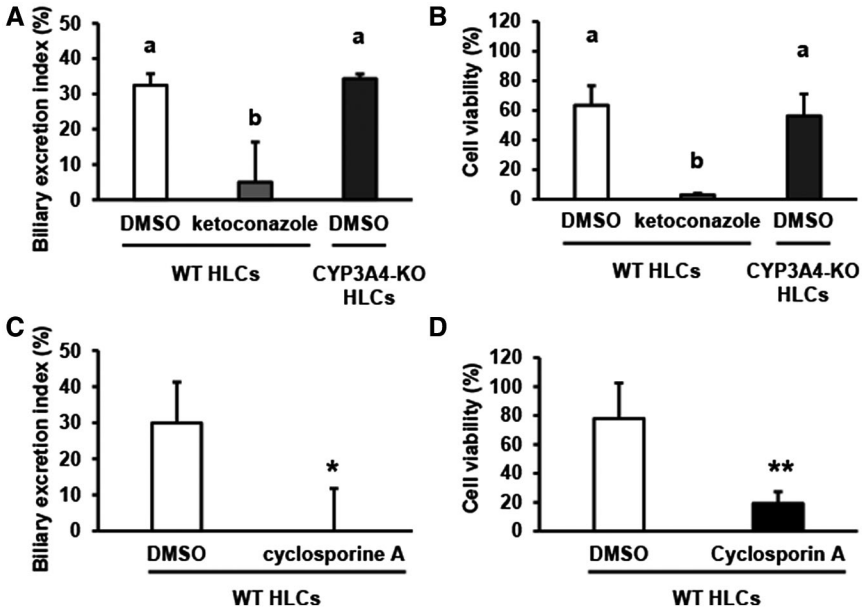

FIG. 5. Off-target effects of ketoconazole. (A,B) HLCs were treated with vehicle (DMSO) or ketoconazole for 24 hours. (A) BEI was calculated in WT HLCs and CYP3A4-KO HLCs to evaluate biliary excretion capacity. Data represent mean ± SD (n = 7). (B) WT HLCs and CYP3A4-KO HLCs were exposed to a BA mixture for 24 hours. Cell viability was examined by WST-8 assay and was calculated as a percentage of cells treated with vehicle only. Data represent mean ± SD (n = 7).Groups that do not share the same letter in (A,B) are significantly different from each other ($P < 0.05$, Tukey's post hoc tests). (C,D) WT HLCs were treated with vehicle (DMSO) or cyclosporine A for 24 hours. (C) BEI was calculated in WT HLCs to evaluate biliary excretion capacity. Data represent mean ± SD (n = 6). (D) HLCs were exposed to a BA mixture for 24 hours. Cell viability was examined by WST-8 assay and was calculated as a percentage of cells treated with vehicle only. Data represent mean ± SD (n = 3). (*$P < 0.05$, **$P < 0.01$, Student's *t*-test).

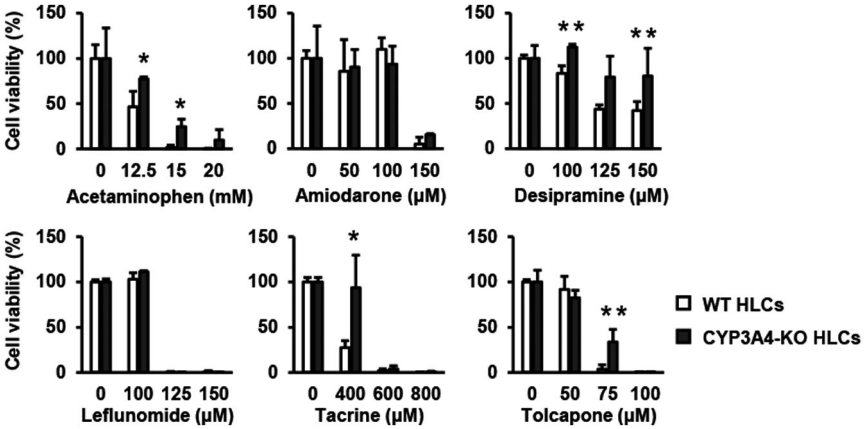

FIG. 6. Prediction of drug-induced liver injury using CYP3A4-KO HLCs. WT HLCs and CYP3A4-KO HLCs were exposed to different concentrations of acetaminophen, amiodarone, desipramine, tacrine, tolcapone, and leflunomide for 4 days. Cell viability of both cell types was examined by WST-8 assay and was calculated as a percentage of cells treated with vehicle only. All data represent mean ± SD (n = 3). (*$P < 0.05$, **$P < 0.01$, Student's *t*-test).

IECs (WT IECs, 3.4×10^4 pmol/hour/mg protein; ketoconazole-treated WT IECs, 3.3×10^2 pmol/hour/mg protein; CYP3A4-KO IECs, 1.4×10^2 pmol/hour/mg protein). These results indicate that CYP3A4-KO IECs decrease CYP3A4 expression and its activity. Finally, to examine whether CYP3A4-KO IECs could

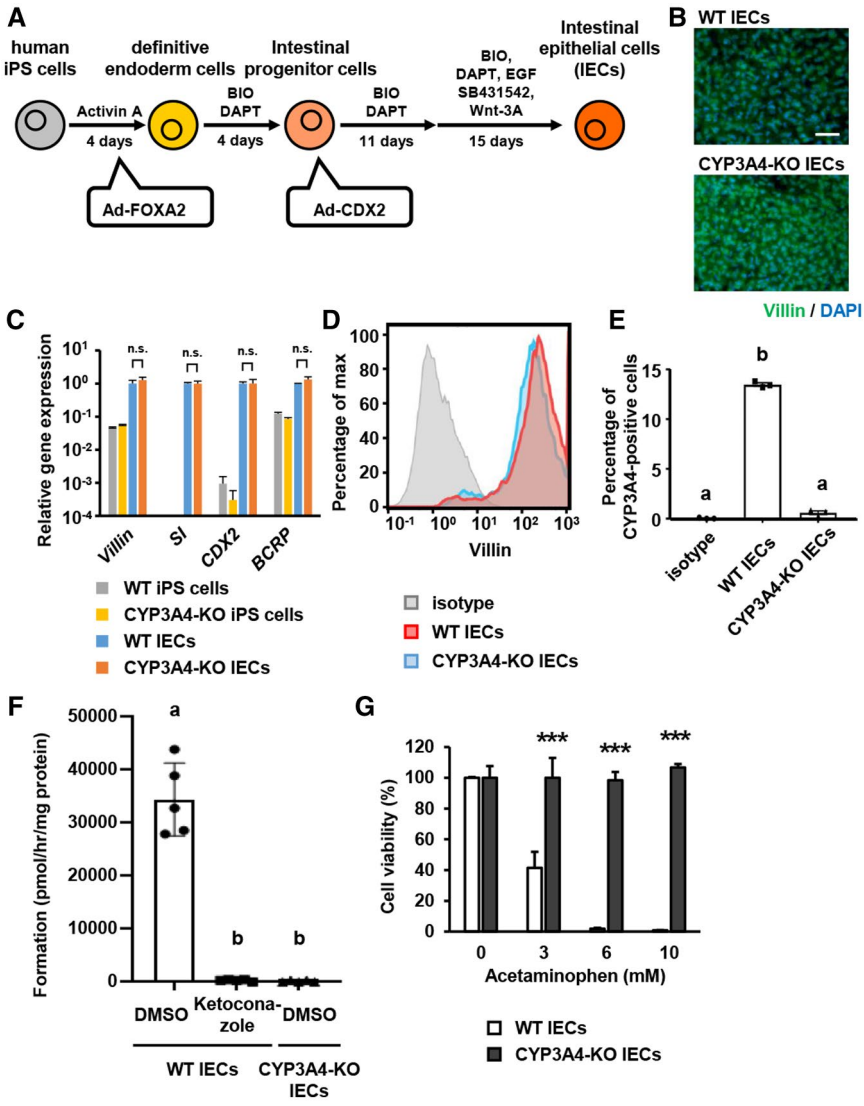

FIG. 7. Characterization of CYP3A4-KO IECs. (A) Schematic overview shows the protocol for intestinal differentiation. (B) WT IECs and CYP3A4-KO IECs were subjected to immunostaining with anti-villin (green) antibodies. Nuclei were counterstained with DAPI (blue). Scale bar, 50 μm. (C) Gene expression levels of villin, *SI*, *CDX2*, and *BCRP* in WT iPS cells, CYP3A4-KO iPS cells, WT IECs, and CYP3A4-KO IECs were examined by real-time RT-PCR. Gene expression levels in WT IECs were taken as 1.0. All data represent mean ± SD (n = 3). (D) Percentage of villin-positive cells in the WT IECs and CYP3A4-KO IECs was measured by using FACS analysis. (E) Percentage of CYP3A4-positive cells in the WT IECs and CYP3A4-KO IECs was measured by using FACS analysis. (F) IECs were treated with vehicle (DMSO) or ketoconazole for 24 hours. CYP3A4-mediated drug-metabolizing capacity in WT IECs and CYP3A4-KO IECs was evaluated by quantifying the metabolites of midazolam by UPLC/MS-MS. Groups that do not share the same letter in (E,F) are significantly different from each other ($P < 0.05$, Tukey's post hoc tests). (G) WT IECs and CYP3A4-KO IECs were exposed to different concentrations of acetaminophen for 4 days. Cell viability was examined by WST-8 assay and was calculated as a percentage of cells treated with vehicle only. All data represent mean ± SD (n = 3). (***$P < 0.005$, Student's *t*-test). Abbreviations: Ad, adenovirus; BIO, 6-bromoindirubin-30-oxime; *BCRP*, breast cancer resistance protein; CDX2, caudal type homeobox 2; DAPT, N-[(3,5-difluorophenyl) acetyl]-Lalanyl-2-phenyl-1, 1-dimethylethyl ester-glycine; EGF, epidermal growth factor; FOXA2, forkhead box A2; hr, hour; n.s., not significant; *SI*, sucrase-isomaltase.

be used in the prediction of drug-induced enterotoxicity, we treated WT IECs and CYP3A4-KO IECs with acetaminophen, which is known to cause enterotoxicity (Fig. 7G).[24] After those cells were exposed to acetaminophen for 4 days, cell viability was measured. Cell viability of CYP3A4-KO IECs

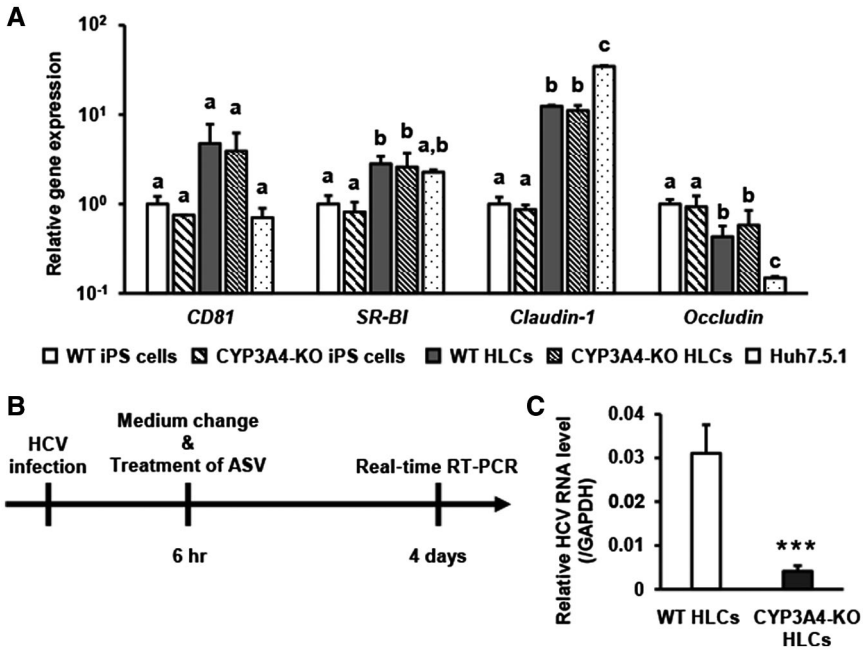

FIG. 8. Evaluation of the therapeutic effects of an anti-HCV drug metabolized by CYP3A4 using CYP3A4-KO HLCs. (A) Gene expression levels of *CD81*, *SR-B1*, claudin-1, and occludin in WT iPS cells, CYP3A4-KO iPS cells, WT HLCs, and CYP3A4-KO HLCs were examined by real-time RT-PCR. Gene expression levels in undifferentiated WT iPS cells were taken as 1.0. Groups that do not share the same letter are significantly different from each other ($P < 0.05$, Tukey's post hoc tests). (B) Schematic overview shows the protocol for HCV infection and treatment with ASV. WT HLCs and CYP3A4-KO HLCs were infected with HCV at an MOI of 0.1. After 6 hours, HLCs were treated with ASV for 4 days. (C) Intracellular HCV genomic RNA levels in WT HLCs and CYP3A4-KO HLCs were determined by real-time RT-PCR. (***$P < 0.005$, Student's *t*-test). Abbreviations: CD81, cluster of differentiation 81; GAPDH, glyceraldehyde 3-phosphate dehydrogenase; hr, hour; MOI, multiplicity of infection; SR-B1, SR-BI scavenger receptor class B type I.

was significantly higher than that of WT IECs, suggesting that CYP3A4-KO IECs could be useful in the prediction of CYP3A4-mediated drug-induced enterotoxicity.

EVALUATION OF THE THERAPEUTIC EFFECT OF AN ANTI-HEPATITIS C VIRUS DRUG METABOLIZED BY CYP3A4, USING HUMAN iPS CELL-DERIVED HLCs

Hepatitis C virus (HCV) infection has a risk of causing chronic hepatitis, cirrhosis, and hepatocellular carcinoma. Direct-acting antivirals (DAAs) are drugs that target HCV proteins, such as nonstructural protein (NS)3/4A protease, NS5A, or NS5B polymerase. DAA therapy succeeded in curing over 90% of patients with chronic hepatitis C.[25] Because most DAAs are metabolized by CYP3A4, their medical effects are affected by the expression fluctuation of CYP3A4.[26] Therefore, we examined whether CYP3A4-KO HLCs could be used to evaluate the anti-viral effects of DAA metabolized by CYP3A4.

First, we examined whether WT HLCs and CYP3A4-KO HLCs express putative receptors for HCV (Fig. 8A). Gene expression levels of cluster of differentiation 81 (*CD81*), scavenger receptor class B type I (*SR-BI*), claudin-1, and occludin were not changed by CYP3A4 KO. Next, to evaluate the anti-viral effects of DAA, we treated WT HLCs and CYP3A4-KO HLCs with asunaprevir (ASV), which is a widely used DAA metabolized by CYP3A4.[27] The procedure used for HCV infection is schematically shown in Fig. 8B. The expression level of the HCV genome was significantly lower in CYP3A4-KO HLCs than in WT HLCs (Fig. 8C). This suggests that the anti-viral effect of ASV was largely affected by CYP3A4 deficiency. Our CYP3A4-KO HLCs could be a model for evaluating the drug–drug interactions of DAAs that are metabolized by CYP3A4.

We also confirmed the anti-viral effects of ASV in HuH7.5.1 cells (a popular model cell line for HCV infection) in the presence or absence of ketoconazole (Supporting Fig. S4). However, the drug-metabolizing capacity of CYP3A4 in Huh7.5.1 is extremely low. Therefore, when an inhibitor or inducer of CYP3A4 coexists, the anti-viral effects of ASV cannot be evaluated in Huh7.5.1 cells. As expected, the expression levels of the HCV genome in Huh7.5.1 cells were not changed by CYP3A4 inhibitor (ketoconazole) treatment. This suggests that it would be useful to evaluate CYP3A4-mediated anti-viral effects of DAAs by using CYP3A4-KO HLCs but not Huh7.5.1 cells.

Discussion

In this study, we succeeded in generating a novel *in vitro* system to evaluate CYP3A4-mediated drug metabolism and drug-induced toxicity using human iPS cells and genome editing technology. This evaluation system was superior to the cell model using ketoconazole (a CYP3A4 inhibitor) treatment because off-target effects, such as the inhibition of BA excretion transporters, were hardly observed in CYP3A4-KO cells but they were observed in ketoconazole-treated cells.

To demonstrate that drug-induced toxicity can be predicted using our evaluation system, a drug-induced toxicity test was conducted using acetaminophen, amiodarone, desipramine, leflunomide, tacrine, and tolcapone (Figs. 6 and 7G). Acetaminophen, amiodarone, desipramine, tacrine, and tolcapone are reportedly metabolized into reactive metabolites by CYP3A4 and have a risk of causing hepatotoxicity. On the other hand, leflunomide was mainly metabolized by CYP2C9 but not by CYP3A4. As expected, hepatotoxicity induced by acetaminophen, desipramine, tacrine, or tolcapone treatment was reduced by CYP3A4 deficiency, while leflunomide-induced hepatotoxicity was not changed by CYP3A4 deficiency (Fig. 6). We also found, in contrast to a previous report,[28] that hepatotoxicity induced by amiodarone was not changed by CYP3A4 deficiency. Amiodarone has a long half-life, and its adverse effects frequently occur through long-term exposure.[29] Therefore, it might be possible to detect amiodarone-induced hepatotoxicity mediated by CYP3A4 by treating HLCs with amiodarone for a long period of time (approximately 2 weeks). Acetaminophen is known to be metabolized by not only CYP3A4 but also CYP2E1.[30] We confirmed that CYP3A4 deficiency completely reduced acetaminophen-induced enterotoxicity of IECs (Fig. 7G) but only partially reduced this in HLCs (Fig. 6). This may be because HLCs but not IECs have CYP2E1 activity (Supporting Fig. S5), and therefore CYP3A4-KO HLCs can still metabolize acetaminophen into reactive metabolites. These results suggest that our evaluation system would be useful for predicting CYP3A4-mediated hepatotoxicity and enterotoxicity.

In addition to the drug-induced toxicity test, we also analyzed the anti-viral effects of a DAA metabolized by CYP3A4. ASV is an NS3 protease inhibitor that can achieve an approximately 85% sustained virological response rate by combined treatment of daclatasvir (NS5A replication complex inhibitor).[31] We compared the anti-viral effect of ASV between WT HLCs and CYP3A4-KO HLCs and found that the anti-viral effect in CYP3A4-KO HLCs was stronger than in WT HLCs (Fig. 8). This might be because a more unchanged form of ASV, which can eliminate HCV, had accumulated in CYP3A4-KO HLCs. We performed a similar experiment with Huh7.5.1 cells, which are widely used as an HCV cell culture infection model, and found that the anti-viral effect of ASV did not change with a CYP3A4 inhibitor (ketoconazole) treatment (Supporting Fig. S4B). This is because CYP3A4 activity in Huh7.5.1 cells was much lower than in human iPS cell-derived HLCs (Supporting Fig. S4A). Therefore, to examine the drug–drug interaction between DAA metabolized by CYP3A4 and a CYP3A4 inhibitor (or inducer), our evaluation system would be much superior to Huh7.5.1 cells. Moreover, human iPS cell-derived HLCs but not Huh7.5.1 cells have the potential to cause a strong innate immune response in the presence of HCV.[32] We suggest, therefore, that human iPS cell-derived HLCs would be a potent model for HCV infection.

It is known that orally administered drugs are absorbed and metabolized in the small intestine and liver and then reach the systemic circulation. In order to predict the first-pass effect of drugs metabolized by CYP3A4, it is necessary to evaluate drug metabolism in the small intestine and liver continuously because CYP3A4 is highly expressed in both organs. Recently, the microphysiological system (MPS), an interconnected set of two- or three-dimensional

cellular constructs, has been developed as a model to perform a pharmacokinetics study mimicking conditions *in vivo*.[33,34] By using MPS technology, it would be possible to combine CYP3A4-KO HLCs with CYP3A4-KO IECs in a single MPS device, which would help us predict the contribution of CYP3A4 to the first-pass effect of orally administered drugs, reproducing the complex tissue responses *in vivo*.

However, these models that include human iPS cell-derived HLCs and IECs have limitations. It takes a longer time (more than 25 days) to generate these cells from undifferentiated human iPS cells than from cell lines such as HepG2, HepaRG, and Caco-2. In addition, human iPS cell-derived HLCs and IECs have a fetal phenotype.[35] Therefore, the results obtained with these models may reflect the fetal rather than adult condition. If adult-type human iPS cell-derived HLCs and IECs can be produced in a short period, it is expected that they will be a useful resource for many pharmaceutical studies.

In this study, we established an *in vitro* system to evaluate CYP3A4-mediated drug metabolism and drug-induced toxicity using human iPS cells and genome editing technology. By using our model, CYP3A4-mediated metabolism and hepatotoxicity of drug candidates would become clear in the early phase of drug development. If drugs that cause toxicity can be eliminated in advance by using an *in vitro* cell model, the risk of unexpected toxicity in animal experiments and clinical trials can be reduced. We hope that our research will help in developing drugs with a lower risk of side effects.

Acknowledgment: We thank Ms. Yasuko Hagihara, Ms. Natsumi Mimura, and Ms. Ayaka Sakamoto for their excellent technical support. The graphical abstract was created using BioRender (https://biorender.com/).

REFERENCES

1) Anzenbacher P, Anzenbacherová E. Cytochromes P450 and metabolism of xenobiotics. Cell Mol Life Sci 2001;58:737-747.
2) Takayama K, Morisaki Y, Kuno S, Nagamoto Y, Harada K, Furukawa N, et al. Prediction of interindividual differences in hepatic functions and drug sensitivity by using human iPS-derived hepatocytes. Proc Natl Acad Sci U S A 2014;111:16772-16777.
3) Takayama K, Inamura M, Kawabata K, Sugawara M, Kikuchi K, Higuchi M, et al. Generation of metabolically functioning hepatocytes from human pluripotent stem cells by FOXA2 and HNF1α transduction. J Hepatol 2012;57:628-636.
4) Negoro R, Takayama K, Kawai K, Harada K, Sakurai F, Hirata K, et al. Efficient generation of small intestinal epithelial-like cells from human iPSCs for drug absorption and metabolism studies. Stem Cell Reports 2018;11:1539-1550.
5) **Takayama K**, **Negoro R**, Yamashita T, Kawai K, Ichikawa M, Mori T, et al. Generation of human iPSC–derived intestinal epithelial cell monolayers by CDX2 transduction. Cell Mol Gastroenterol Hepatol 2019;8:513-526.
6) Takayama K, Igai K, Hagihara Y, Hashimoto R, Hanawa M, Sakuma T, et al. Highly efficient biallelic genome editing of human ES/iPS cells using a CRISPR/Cas9 or TALEN system. Nucleic Acids Res 2017;45:5198-5207.
7) Takayama K, Hagihara Y, Toba Y, Sekiguchi K, Sakurai F, Mizuguchi H. Enrichment of high-functioning human iPS cell-derived hepatocyte-like cells for pharmaceutical research. Biomaterials 2018;161:24-32.
8) Deguchi S, Yamashita T, Igai K, Harada K, Toba Y, Hirata K, et al. Modeling of hepatic drug metabolism and responses in CYP2C19 poor metabolizer using genetically manipulated human iPS cells. Drug Metab Dispos 2019;47:632-638.
9) **Kawai K**, **Negoro R**, Ichikawa M, Yamashita T, Deguchi S, Harada K, et al. Establishment of SLC15A1/PEPT1-knockout human-induced pluripotent stem cell line for intestinal drug absorption studies. Mol Ther - Methods Clin Dev 2020;17:49-57.
10) **Cong L**, **Ran FA**, Cox D, Lin S, Barretto R, Habib N, et al. Multiplex genome engineering using CRISPR/Cas systems. Science 2013;339:819-823.
11) Li H, Fujimoto N, Sasakawa N, Shirai S, Ohkame T, Sakuma T, et al. Precise correction of the dystrophin gene in duchenne muscular dystrophy patient induced pluripotent stem cells by TALEN and CRISPR-Cas9. Stem Cell Reports 2015;4:143-154.
12) The ChEMBL-OG. Withdrawn drugs. http://chembl.blogspot.com/2018/06/withdrawn-drugs.html. Published June 12, 2018. Accessed January 2020.
13) Van Waterschoot RAB, Van Herwaarden AE, Lagas JS, Sparidans RW, Wagenaar E, Van Der Kruijssen CMM, et al. Midazolam metabolism in cytochrome P450 3A knockout mice can be attributed to up-regulated CYP2C enzymes. Mol Pharmacol 2008;73:1029-1036.
14) Sanoh S, Tamura Y, Fujino C, Sugahara G, Yoshizane Y, Yanagi A, et al. Changes in bile acid concentrations after administration of ketoconazole or rifampicin to chimeric mice with humanized liver. Biol Pharm Bull 2019;42:1366-1375.
15) Morgan RE, Trauner M, van Staden CJ, Lee PH, Ramachandran B, Eschenberg M, et al. Interference with bile salt export pump function is a susceptibility factor for human liver injury in drug development. Toxicol Sci 2010;118:485-500.
16) Susukida T, Sekine S, Nozaki M, Tokizono M, Oizumi K, Horie T, et al. Establishment of a drug-induced, bile acid-dependent hepatotoxicity model using HepaRG cells. J Pharm Sci 2016;105:1550-1560.
17) Ogimura E, Tokizono M, Sekine S, Nakagawa T, Bando K, Ito K. Metabolic activation of cholestatic drug-induced bile acid-dependent toxicity in human sandwich-cultured hepatocytes. J Pharm Sci 2017;106:2509-2514.
18) **Jiang Y**, **Fan X**, Wang Y, Chen P, Zeng H, Tan H, et al. Schisandrol B protects against acetaminophen-induced hepatotoxicity by inhibition of CYP-mediated bioactivation and regulation of liver regeneration. Toxicol Sci 2015;143:107-115.
19) Takai S, Oda S, Tsuneyama K, Fukami T, Nakajima M, Yokoi T. Establishment of a mouse model for amiodarone-induced liver injury and analyses of its hepatotoxic mechanism. J Appl Toxicol 2016;36:35-47.

20) Morrow PL, Hardin NJ, Bonadies J. Hypersensitivity myocarditis and hepatitis associated with imipramine and its metabolite, desipramine. J Forensic Sci 1989;34:1016-1020.
21) McEneny-King A, Osman W, Edginton AN, Rao PPN. Cytochrome P450 binding studies of novel tacrine derivatives: predicting the risk of hepatotoxicity. Bioorg Med Chem Lett 2017;27:2443-2449.
22) Smith KS, Smith PL, Heady TN, Trugman JM, Harman WD, Macdonald TL. In vitro metabolism of tolcapone to reactive intermediates: relevance to tolcapone liver toxicity. Chem Res Toxicol 2003;16:123-128.
23) Sevilla-Mantilla C, Ortega L, Agúndez JAG, Fernández-Gutiérrez B, Ladero JM, Díaz-Rubio M. Leflunomide-induced acute hepatitis. Dig Liver Dis 2004;36:82-84.
24) Chopyk DM, Stuart JD, Zimmerman MG, Wen J, Gumber S, Suthar MS, et al. Acetaminophen intoxication rapidly induces apoptosis of intestinal crypt stem cells and enhances intestinal permeability. Hepatol Commun 2019;3:1435-1449.
25) Leroy V, Angus P, Bronowicki J-P, Dore GJ, Hezode C, Pianko S, et al. Daclatasvir, sofosbuvir, and ribavirin for hepatitis C virus genotype 3 and advanced liver disease: a randomized phase III study (ALLY-3+). Hepatology 2016;63:1430-1441.
26) Banerjee D, Reddy KR. Review article: safety and tolerability of direct-acting anti-viral agents in the new era of hepatitis C therapy. Aliment Pharmacol Ther 2016;43:674-696.
27) Gong J, Eley T, He B, Arora V, Philip T, Jiang H, et al. Characterization of ADME properties of [(14)C]asunaprevir (BMS-650032) in humans. Xenobiotica 2016;46:52-64.
28) Wu Q, Ning B, Xuan J, Ren Z, Guo L, Bryant MS. The role of CYP 3A4 and 1A1 in amiodarone-induced hepatocellular toxicity. Toxicol Lett 2016;253:55-62.
29) Epstein AE, Olshansky B, Naccarelli GV, Kennedy JI, Murphy EJ, Goldschlager N. Practical management guide for clinicians who treat patients with amiodarone. Am J Med 2016;129:468-475.
30) McGill MR, Jaeschke H. Metabolism and disposition of acetaminophen: recent advances in relation to hepatotoxicity and diagnosis. Pharm Res 2013;30:2174-2187.
31) Kumada H, Suzuki Y, Ikeda K, Toyota J, Karino Y, Chayama K, et al. Daclatasvir plus asunaprevir for chronic HCV genotype 1b infection. Hepatology 2014;59:2083-2091.
32) **Sakurai F**, **Kunito T**, Takayama K, Hashimoto R, Tachibana M, Sakamoto N, et al. Hepatitis C virus-induced innate immune responses in human iPS cell-derived hepatocyte-like cells. Virus Res 2017;242:7-15.
33) Wikswo JP. The relevance and potential roles of microphysiological systems in biology and medicine. Exp Biol Med (Maywood) 2014;239:1061-1072.
34) Tsamandouras N, Chen WLK, Edington CD, Stokes CL, Griffith LG, Cirit M. Integrated gut and liver microphysiological systems for quantitative in vitro pharmacokinetic studies. AAPS J 2017;19:1499-1512.
35) **Baxter M**, **Withey S**, **Harrison S**, Segeritz C-P, Zhang F, Atkinson-Dell R, et al. Phenotypic and functional analyses show stem cell-derived hepatocyte-like cells better mimic fetal rather than adult hepatocytes. J Hepatol 2015;62:581-589.

Author names in bold designate shared co-first authorship.

Supporting Information

Additional Supporting Information may be found at onlinelibrary.wiley.com/doi/10.1002/hep4.1729/suppinfo.